Pulse-train modulation in a picosecond self-mode-locked laser

2009 J. Phys. B: At. Mol. Opt. Phys. 42 145402

(http://iopscience.iop.org/0953-4075/42/14/145402)

J. Phys. B: At. Mol. Opt. Phys. **42** (2009) 145402 (6pp) doi:10.1088/0953-4075/42/14/145402

Pulse-train modulation in a picosecond self-mode-locked laser

Chih-Chang Hsu[1], **Ja-Hon Lin**[2] **and Wen-Feng Hsieh**[1,3]

[1] Department of Photonics and Institute of Electro-Optical Engineering, National Chiao Tung University, 1001 Tahsueh Rd, Hsinchu 30050, Taiwan

[2] Department of Electro-Optical Engineering, National Taipei University of Technology, 1, Sec 3, Chung-Hsiao E Rd, Taipei 106, Taiwan

E-mail: wfhsieh@mail.nctu.edu.tw

Received 4 December 2008, in final form 3 April 2009
Published 18 June 2009
Online at stacks.iop.org/JPhysB/42/145402

Abstract

Pulse-train modulation was observed in a picosecond self-mode-locked Ti:sapphire laser with pump-power dependence when it was operated around the degenerate cavity configuration. By increasing the optical pumping power, the envelope of the periodic amplitude modulation splits into two or three clusters with enhanced modulation depth, and the amplitude modulation eventually becomes disordered at higher pump power. The amplitude modulation may be supported by exciting two sets of non-degenerate longitudinally mode-locked supermodes due to spatially inhomogeneous gain modulation in the Ti:sapphire crystal.

1. Introduction

Self-mode-locked lasers due to Kerr-lens mode locking (KLM) have become the light sources of high-bandwidth ultrashort pulses and have been applied to various fields. Recently, the supercontinuum (SC) or white light generation has been demonstrated by injecting the high peak power laser pulses into a photonic crystal fibre (PCF) [1]. By operating the mode-locked Ti:sapphire laser in a pulse-train amplitude modulation mode, the so-called self-Q-switched mode [2] to enhance the peak power, the fluctuating structure of SC spectrum can be suppressed significantly [3]. This Q-switching mode-locking pulse train with low repetition rate is very useful for preventing thermal heating in Z-scan and nonlinear optical measurements [4–6].

The solid-state laser media that usually have sufficient long gain relaxation time as compared with the cavity relaxation time are susceptible to intensity spiking and exhibit self-Q-switching phenomena. Accordingly, introducing extra loss in the laser cavity such as saturable absorbers or semiconductor saturable absorber mirrors (SESAM) can generate self-Q-switching, Q-switched mode locking (QML) and even continuous-wave (CW) mode-locked laser pulses [7, 8]. Although the gain relaxation time of the Ti:sapphire laser (3.2 μs) is larger than the cavity relaxation time (∼10 ns), the mode-locked pulse train in a femtosecond (fs) Ti:sapphire laser can be amplitude modulated by high-order spatial transverse modes [2, 9, 10] or high-order solitons [11] without saturable absorbers. By controlling intracavity hard aperture [9] or operating parameter of the cavity, such as moving spherical mirror or translating prism [2, 10, 11], the intensity dependence of the transverse distribution of the laser beam caused by self-focusing imposes a strong limit on the aperture diameter. When the size of an intracavity slit is reduced below its optimal value for stable mode locking, the output pulses of the KLM Ti:sapphire laser transform into a regime characterized by periodic pulse-train amplitude modulations as a kind of repetitive self-Q-switching. The modulation period increased and amplitude modulation could deepen to almost 100% as the slit width was decreased further [9]. The period of self-Q-switching depends on the distance between the folding mirrors, which essentially determine the stability of resonator, and increases with increasing the distance between one of the folding mirrors and the closer face of the Ti:sapphire crystal [10]. Among them, the high-order transverse modes, strong Kerr effect due to the ultrashort pulsewidth and the group velocity dispersion (GVD) compensation should be responsible to the mode-locked pulse-train modulation in the fs Ti:sapphire lasers.

In contrast, due to the relatively low peak intensity in picosecond (ps) KLM lasers, the strength of the Kerr effect is reduced and therefore the pulse-train modulation should occur more difficult than that in fs-KLM lasers. However,

[3] Author to whom any correspondence should be addressed.

because the mode-locking mechanism of the KLM laser is due to the self-amplitude or self-gain modulation resulting from the self-focused light by hard or soft aperture effect, the smaller pumped beam spot size than the cold cavity beam one in the gain medium leads to the KLM mode resonating more easily than the CW mode. In an axially tightly focused pumped laser, it is easier to excite the higher order transverse modes to extract more stored energy from the gain medium when the laser is operated in the degenerate cavity configurations [12] that have the so-called low-order resonance [13]. The beam patterns observed for both the cw and picosecond KLM operations in the soft aperture KLM regions are no longer pure fundamental Gaussian modes [12]. Due to the competition of transverse modes, the nonlinear dynamics and irregular pulsing have been observed in Nd:YVO_4 lasers [14] and Ti:sapphire lasers [15] operated around the degeneration configurations. Furthermore, the optical Kerr effect can be exploited to mimic the fast saturable absorber, and the rate-equation approach is sufficient to explain the transmission of an optical pulse through such a fast saturable absorber without using more complex resonant-dipole or Rabi-flopping analyses [16]. In this paper, we report the observation and simulation, using the Collin's integral with the rate equations [17], of the periodic amplitude modulation of ps-mode-locking pulses occurring around the 1/3-degenerate configuration, which corresponds to the 1/4-fractional low-order resonance. The slow amplitude modulation of the mode-locked pulse train in the ps-soft-aperture self-mode-locked Ti:sapphire laser depends upon the optical pumping power. As the pump power increases, the envelope of the periodic modulation will split into two or three clusters, and the laser eventually turns into disorder modulation as further increasing the pump power.

2. Experimental details

The schematic experimental setup of the ps-KLM Ti:sapphire laser is shown in figure 1, which is a z-folded four-mirror cavity containing a 9 mm-long Brewster-cut Ti:sapphire rod (Ti^{3+}: 0.1% doped, FOM > 150) without any hard-aperturing slit and group-velocity compensation components. A CW frequency doubled Nd:YVO_4 laser (Coherent, Verdi-V8) was used as the pumped source, and the pumped beam is focused by a plano-convex lens with focal length of 12.7 cm at the centre of the laser rod. Two curved mirrors (M_1 and M_2) of 10 cm radius of curvature were tilted about 10° angle to compensate the astigmatism. The distance r_2 from curved mirror M_1 to one endface of the laser rod is 52.85 mm, and the distance r_1 from the other endface to curved mirror M_2 is tunable from 52.80 mm to 52.89 mm. Two flat mirrors, a 98% high reflector M_3 and a 95% output coupler M_4, were placed to form linear arms. The distance between M_1 and M_4, as well as the distance between M_2 and M_3, is 75 cm to form a near-symmetric cavity arrangement. The total length of the resonator is approximately 160 cm, resulting in an axial mode spacing of 93.3 MHz. The lens, the laser rod and the folding mirrors were mounted on precision translation stages with precision of 10 μm to allow for fine adjustment of the resonator configuration and the overlap between pumped beam and cavity beam. The cold-cavity beam diameter at the centre of the laser rod corresponds to 50 μm, which is larger than the pump one of 30 μm. The laser beam from the high reflector M_3 was detected by two high-speed photodetectors with rise time < 0.3 ns and noise equivalent power 10^{-13} W $Hz^{-1/2}$. The output signals of photodetectors were sent to a LeCroy-9450 A digital oscilloscope (300 MHz bandwidth) and a RF spectrum (HP 8560E) for monitoring the pulse sequence and the dynamics of the Ti:sapphire laser. A CCD camera was used for observing the transverse pattern of the laser beam. The beam patterns observed for both the cw and picosecond KLM operations around the degenerated configuration are no longer pure fundamental Gaussian modes which consist of several high-order Hermite–Gaussian modes with phase shifts relative to the fundamental one [12]. The inset of figure 1 shows the beam pattern around the 1/3-degenerate cavity configuration.

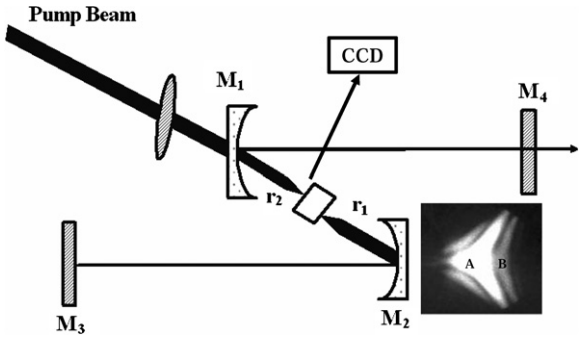

Figure 1. The schematic experimental setup of the Kerr-lens mode-locking Ti:sapphire laser. The inset of figure 1 showed the beam pattern around the 1/3-degenerate cavity configuration.

3. Results and discussion

The pumping threshold of mode locking is about 3 W. We can operate the laser in the picosecond mode locking with central wavelength of 820 nm at pump power P_p = 4 W at the cavity length slightly longer than the 1/3-degenerate cavity configuration by properly tuning the mirror M_2 (~100 μm tuning range) after a mechanical perturbation [12, 18]. When the curved mirror M_2 was translated slightly towards increasing the cavity length (~15 μm), the sinusoidal amplitude modulation of the mode-locking pulse train was observed as shown in figure 2(a). We kept increasing the distance of r_1, the pulse-train modulation presented intermittent modulation behaviours varying among figures 2(b)–(d). By further increasing the distance of r_1, self-starting mode locking (within 30 μm tuning range) was observed, finally, the laser turned to CW output.

By increasing the pump power from 4 W to 5 W, we observed the pulse-train modulation progressively changed from the sinusoidal amplitude modulation state of figure 2(a) to figures 2(b)–(d). The modulation rate was estimated approximately at 250 kHz and the modulation depth was about 50% in figure 2(a). As the pump power is increased, the modulation rate increases and each of the self-Q-switch

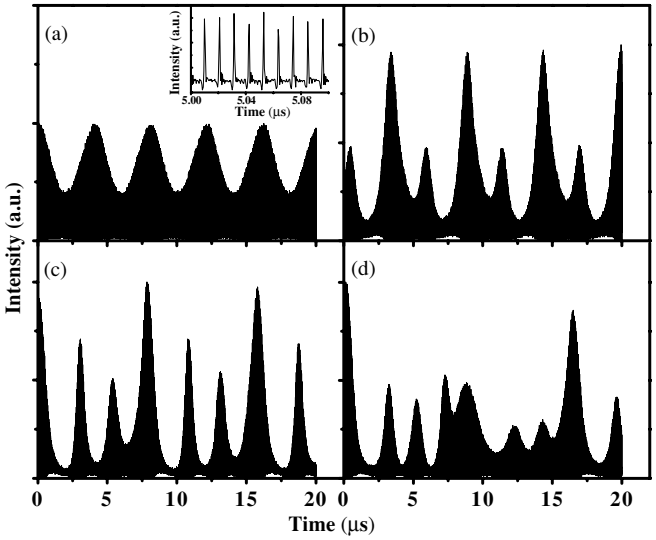

Figure 2. Power-dependent mode-locked pulse-train modulations: (a) periodic modulation pulse train with 4 W pump power; (b) the modulation envelope splits into two clusters with 4.2 W pump power; (c) the modulation envelope splits into three clusters with 4.5 W pump power and (d) irregular modulation of pulse-train with 5 W pump power. The inset shows the mode-locked pulses inside the modulation envelope.

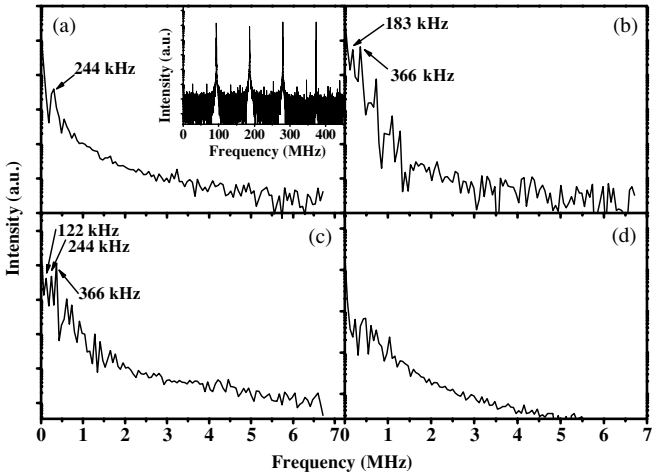

Figure 3. The expanded power spectra of different modulation states of figure 2 around the central frequency 93.3 MHz. Inset shows the power spectrum in the coarse scale to the repetition frequency of 93.3 MHz.

pulses progressively splits into period-two at $P_p = 4.2$ W, period-three at $P_p = 4.5$ W, and then becomes irregular at $P_p = 5$ W as shown in figures 2(b)–(d), respectively. We also observed that there is a period-doubling route to chaos with increasing pump power. Note that the mode-locked pulses within the modulation envelope as in the inset of figure 2(a) show that each of the individual mode-locked pulses does not split due to the high-order solitons [11, 19] in any cases of the above-mentioned pulse-train modulation, because the optical Kerr effect in the picosecond Ti:sapphire laser may not be strong enough to induce pulse-splitting behaviour [20]. Furthermore, the filtering mechanism from the loss difference [19, 20] need not be considered because the gain bandwidth of the picosecond pulses is much smaller than the bandwidth of mirror reflectance.

The extended power spectra of different modulation states of figure 2 look alike as shown in the inset of figure 3(a) with the repetition rate remaining ∼93.3 MHz. We then further expanded the power spectra of the pulse-train modulations at the central frequency 93.3 MHz and shown in figures 3(a)–(d). The beat frequency located beside the central frequency corresponds to the pulse-train modulation frequency. The frequency of the periodic modulation is 244 kHz, which agrees with the estimated 250 kHz from oscilloscope trace in figure 2(a). As pumping increases, the modulation frequency increases first to become 366 kHz with subharmonic at 188 kHz (see figure 3(b)) in the period-two modulation as the time trace in figure 2(b); and then to become 366 kHz with period-three beating of 122 kHz and 244 kHz as shown in figure 3(c). The modulation becomes irregular with no dominant peaks in figure 3(d) on further increasing the pump power.

Because the upper-state lifetime of the Ti:sapphire crystal is 3.2 μs and the laser threshold is about 3 W, we estimated the relaxation oscillation frequency to be about 229 kHz [21]. A detailed theoretical study of self-Q switching was performed by Haus [22]. The frequency that corresponds to the several-microsecond period of self-Q-switching is close to the relaxation oscillation frequency, which can be explained by the nonlinear interaction between the population inversion in the gain medium and the optical-field intensity in the cavity. However, since M_2 is translated only by 15 μm and the parameters, such as the beam waist of the cold cavity, cavity loss, etc, are almost unchanged, the modulation behaviour is not induced by cavity loss. Therefore, the modulation mechanism should not be only Q-switching. In addition, in a femtosecond Ti:sapphire laser, soliton-like pulse shaping is dominant by balancing the self-phase modulation (SPM) in the Ti:sapphire rod and the net negative group velocity dispersion provided by prism pair or chirped mirrors. Because GVD compensation prisms are absent in our picosecond mode-locked Ti:sapphire, the laser pulses would not form solitons. Therefore, the modulation mechanism should be different from that of Tsang's paper [11]. Also, unlike Liu's [9] or Xing's [2] resonator setups, our picosecond mode-locked laser is based on the soft-aperture effect in the Ti:sapphire crystal instead of using a hard aperture.

However, in an axially pumped laser, especially for the soft-aperture KLM laser with the pump size less than the cavity beam size, it is easy to excite the higher order transverse modes to extract more stored energy from the gain medium when the laser is operated in the degenerate cavity [12]. The slow amplitude modulation of the mode-locked pulse train may be due to the transverse modes interaction. For verification, we have used two small-area detectors to measure intensities at different transversal positions of the pattern labelled A and B in the inset of figure 1. Figure 4 shows the intensities of the laser simultaneously detected at two transversal positions. Not only both of the period-two pulse trains but also inverse evolution was observed at positions A and B, revealing that the transverse pattern is non-stationary and exhibits a spatial–temporal instability. Therefore, the

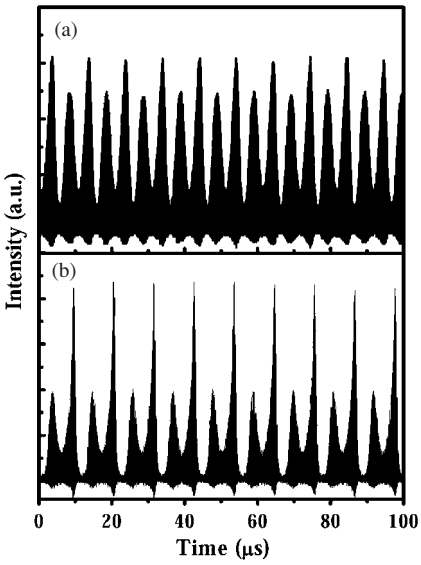

Figure 4. The simultaneous intensities of the laser at two transversal positions labelled A and B in the inset of figure 1.

slow pulse-train amplitude modulation should be dominated by transverse modes interaction rather than longitudinal modes interaction.

Typically, if only one spatial mode of the electromagnetic field is excited in the laser, the interesting instabilities are temporal [23, 24]. Nevertheless, under some circumstances, parameters can be adjusted so that more spatial modes come into play and spatio-temporal instabilities [25] also appear. Lugiato *et al* expressed the Maxwell–Bloch equations in terms of modal amplitudes by using a suitably cylindrically symmetric empty-cavity-mode expansion [26, 27]. They presented a variety of spatio-temporal instabilities, including chaos and cooperative frequency locking, which occur under uniform and low-power pumped, by tuning the mode spacing. They were able to do this because the Laguerre–Gaussian modes are a set of good bases only when the uniform-field limit is applied for a so-called good cavity with small gain. Thus, their results are valid only for a laser in which the pump size is larger than the minimum cavity beam waist [28]. However, in axial-continuously (CW) pumped lasers, gain saturation provides an inherently nonlinear effect and when the pump size is smaller than the waist of the cold cavity, peculiar lasing behaviours [14, 29–32] have been observed in an end-pumped solid-state laser near the degenerate configurations that correspond to the low-order resonance. At these degenerate cavity configurations, because of the superposition of high-order degenerate modes, the transverse mode pattern can be self-adjusted to match the pumping profile for extracting maximal pumped gain in the cavity, a supermode or superposition of phase-locked degenerate transverse modes can be formed with relatively low lasing threshold. Beam waist shrinkage [30] and operation of a stable CW bottle beam [31, 32] were observed around the degenerate cavities. As in our previous report [17], under tightly axially pumped, the laser would possess spatio-temporally instability if the cavity length is detuned away longer than that of the degenerates. We believe that the detuning of the cavity from the degenerates may result in excitation of another supermode due to spatially inhomogeneous gain. This new supermode is no longer degenerate with the fundamental mode but has a frequency shift corresponding to the Guoy phase. We estimated the length detuning length of the cavity is ∼15 μm. Therefore, we believe that the amplitude modulation may result from competition of these two sets of longitudinally mode-locked supermodes, which no longer can be phase locked by gain saturation.

Because in the Kerr-lens mode-locked laser, the optical Kerr effect can be exploited to simulate the fast saturable absorber behaviour, and the rate-equation approach can describe sufficiently the transmission of an optical pulse through such a fast saturable absorber [16]. Here, we simulated the slow amplitude modulation behaviour of this picosecond Kerr-lens Ti:sapphire laser based on the Fox-Li's approach, including the self-focusing effect and using the Collin's integral with the rate equations [17]. In a thin-slab approximation [16], we calculate transverse light field distribution $E(r)$ propagating in this laser system by using cylindrical symmetry Collin's integral with transmission matrix $\begin{bmatrix} A & B \\ C & D \end{bmatrix}$, as shown in equation (1)

$$E_m^-(r) = \frac{2\pi \mathrm{j}}{B\lambda}\int_0^a \exp(-\mathrm{j}k2d')E_m^+(r')\exp[-(\mathrm{j}\pi/B\lambda)] \times (Ar'^2 + Dr^2)]J_0(2\pi rr'/B\lambda)r'\mathrm{d}r'. \quad (1)$$

Here $E_m^+(r)$ and $E_m^-(r)$ are the transverse electric fields of the mth round trips at the planes immediately after and before the gain medium (denoted by the superscripts + and −); r and r' are the corresponding radial coordinates, λ is the wavelength of laser, k is the wave number of the laser, d' is the propagating distance, J_0 is a Bessel function of zero order; and a is the aperture radius on the reference plane and it must be chosen large enough with many times of the fundamental mode radius to ensure that the diffraction loss can be neglected.

The rate equations are as described in our previous work [17], in which the gain coefficient is expressed as

$$g_{m+1} = (1 - \gamma_a \Delta t)g_m + \frac{2\Delta t}{h\nu_p N_0 l}\left(\frac{P_p}{\pi w_p^2}\mathrm{e}^{\frac{-2r^2}{w_p^2}}\right) \times (\sigma N_0 - g_m) - \frac{\gamma_a \Delta t}{|E_s|^2}|E_m|^2 g_m. \quad (2)$$

Here we used the spontaneous decay rate $\gamma_a = 3.125 \times 10^5\ \mathrm{s}^{-1}$ [33], the total density $N_0 = 3.3 \times 10^{25}\ \mathrm{m}^{-3}$ [33], the length $l = 9$ mm, the stimulated-emission cross section $\sigma = 3.0 \times 10^{-23}\ \mathrm{m}^2$ [34] and the saturation parameter $E_s = 1.05 \times 10^6\ \mathrm{NC}^{-1}$ [34] of the active medium; and the round trip time $\Delta t = 10.67$ ns that was determined by cavity length, the photon energy of the pumped laser $h\nu_p = 1.53$ eV, pumped beam radius $w_p = 15\ \mu$m in the gain medium and P_p is the effective pump power. Note that the mode locking mechanism in the Kerr-lens mode-locking laser is due to the self-amplitude or self-gain modulation resulting from the self-focused light by hard or soft aperture effect. Therefore, the pumped beam radius w_p must be smaller than the cold cavity beam radius w_c (∼25 μm) in the gain medium, leading to the KLM mode

resonating more easily than the CW mode. We have omitted the dispersion of the active medium so that the gain is assumed to be real. The filtering mechanism from the loss difference [19, 20] need not be considered because the gain bandwidth of the picosecond pulses is much smaller than the bandwidth of mirror reflectance.

In order to include the self-focusing effect in the active medium, we modified the equation to describe the light field passing through the gain medium by adding the nonlinear phase shift caused by the optical Kerr effect

$$\phi(r) = \frac{2\pi}{\lambda} n_2 l I(r), \tag{3}$$

in the evolution equation of the transverse light field:

$$E_m^+(r) = E_m^-(r) \exp\left(\tfrac{1}{2} g_m(r) l - \mathrm{i}\phi(r)\right) + E_{\text{spont}}^m. \tag{4}$$

Here l is the length of gain medium, E_{spont}^m is the field of spontaneous emission whose amplitude is given by the spontaneous decay term in equation (2) and a phase obtained from a random generator; and n_2 is the nonlinear refractive index. $I(r)$ is the intensity distribution of laser pulse calculated from the electric field $E_m^-(r)$ using $I(r) = (1/2n\varepsilon_0)|E_m^-(r)|^2$, where n is the refractive index and ε_0 is permittivity of free space. Similar treatment is used for the opposite direction propagation. When we considered equation (4) without self-focusing effect, equations (2) and (4) can be used to model the laser dynamics with the beam-propagation dominant as cavity is far from degeneration but with interplay of beam propagation and gain dynamics as the cavity is tuned towards degeneration [17]. However, if we considered the self-focusing effect, act as a so-called Kerr lens, it changes the electric field distribution and shrinks the spot size of the electric field to modify the gain profile and to result in the KLM mode resonates more easily than the CW mode.

Note that the light field in the cavity can be expanded as the linear combination of the Hermite–Gaussian or Laguerre–Gaussian transverse modes, the light field in equation (4) presents the superposition of the transverse modes [35]. We calculated the laser output power by integrating the intensity distribution of laser pulse $I(r)$ with respect to the aperture radius a on the reference plane every roundtrip. The processes repeat in each roundtrip until they reach convergence to a continuous-wave steady state for the CW laser output. We varied r_1 that changes the electric field distribution in the gain medium corresponding to influence the optical Kerr effect on laser dynamics across the point of degeneration ($r_1 = 53.625$ mm), and set the initial values of $E(r)$ to zero, i.e., $E_1^-(r) = 0$, to calculate the output power. Here setting the initial values of $E(r) = 0$ is to avoid the value of the stable output field at position r_1 substituted into the initial value at the next position of r_1, and the real initial condition is the spontaneous emission noise rather than 'the zero field value'. All parameters and variables used in the program have been set at double precision.

Figure 5 shows the simulated output power with changing the effective pump power P_p from 4 W to 5 W with and without nonlinear refractive index n_2. By setting the nonlinear index $n_2 = 0$, we found that evolution of laser output is always continuous after relaxation oscillation, as shown in figure 5(a), for the cavity was set for $r_1 = 53.620$–53.645 mm and P_p from

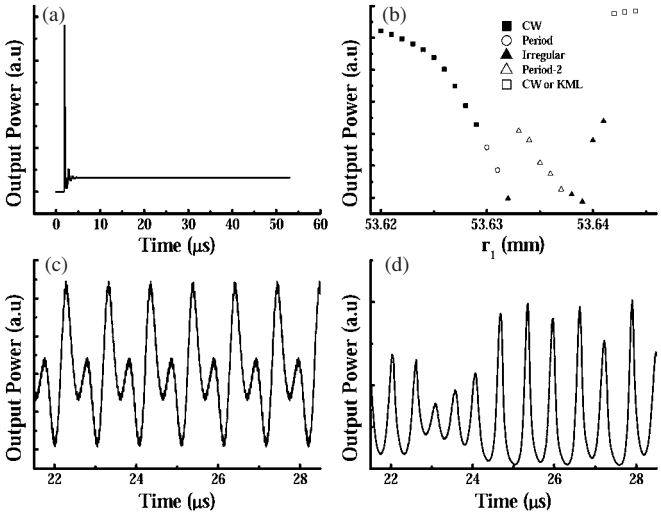

Figure 5. The simulated evolution of output power with changing pump power from 4 W to 5 W with and without Kerr effect. (a) It always shows continuous output after relaxation oscillation over the calculated cavity configurations without Kerr effect ($n_2 = 0$); with Kerr effect on $n_2 = 3 \times 10^{-20}$ m^2 W^{-1}, (b) the cavity tuning region of various dynamic behaviours (e.g., period, period-2, irregular, etc, labelled in the inset) around the degenerated configuration at $P_p =$ 4 W, (c) period-two and (d) irregular pulse-train modulation at $r_1 =$ 53.635 mm with $P_p = 4$ W and 4.5 W, respectively.

4 W to 5 W. However, let $n_2 = 3 \times 10^{-20}$ m^2 W^{-1}, pulsewidth $\tau_p = 3$ ps and $P_p = 4$ W, the laser output power versus r_1 (figure 5(b)) shows the region of various states such as CW output (solid squares), period modulation (open circles) and irregular modulation (solid triangles), etc. When r_1 is smaller than 53.629 mm the laser output presents CW output (solid squares). However, we cannot determine directly whether the constant output is completely KLM or CW output due to lack of temporal information within a roundtrip time and mechanical perturbation term. The simulated time sequence of output power in the unit of roundtrip time corresponds to the envelope amplitude in figure 2. The period modulation state (open circles), whose envelope is similar to figure 2(a), is located between $r_1 = 53.630$ mm and 53.631 mm; the period-two modulation state (open triangles) is at 53.633 mm $< r_1 <$ 53.637 mm; and the irregular modulation state (solid triangles) is at $r_1 = 53.632$ mm and 53.638 mm $< r_1 <$ 53.641 mm; and the laser output may become CW or KLM (open squares) at $r_1 >$ 53.642 mm. Although due to the lack of temporal information within a roundtrip time, we cannot determine directly whether the constant output is self-starting KLM or CW output, we would expect observing self-starting KLM then CW output as known from the experimental observation. The simulated pulse-train modulation with varying r_1 was similar to our observation and the character of the output power dip was similar to [12].

At the position deviating from the degeneration, $r_1 =$ 53.635 mm, the pulse-train amplitude modulation changed from period-two to irregular for pump power being 4 W and 4.5 W respectively, as shown in figures 5(c) and (d), which are similar to figures 2(b) and (d). The amplitude modulation frequency is about 750 kHz in figure 5(c). Owing

to the fact that the pump power in the simulation may be higher than the actual one, the amplitude modulation frequency of the simulation is larger than the measured modulation frequency. Furthermore, in our previous reports [12, 36], the transverse mode pattern consisted of high-order transverse modes around the degenerate cavity configuration. Because of the superposition of high-order modes, the transverse mode could be self-adjusted to match the pumping profile for extracting the maximal pumped gain in the cavity. The optical Kerr effect played a role that enhanced beam waist shrinkage and supermodes generation as the small pump spot size. Therefore, the subharmonic amplitude modulation may result from competition of these sets of longitudinally mode-locked supermodes, which no longer can be phase locked by gain saturation.

4. Conclusion

We have observed slow pulse-train amplitude modulation phenomena in a self-mode-locked picosecond Ti:sapphire laser. Periodic pulse-train modulation appeared when the pump power reached 4 W. As the pump power is increased further, each modulation envelope splits into two or three clusters with increasing modulation depth; and the laser would eventually lead to an irregular modulation pulse train if the pump power were increased even further. The observed irregular pulse envelope modulation is spatio-temporal with non-stationary transverse pattern. The slow amplitude modulation should be supported by exciting two sets of non-degenerate longitudinal mode-locked supermodes due to spatially inhomogeneous gain modulation in the Ti:sapphire crystal.

Acknowledgment

This work is supported by the Natural Science Council of Taiwan, Republic of China, under grant NSC 96-2628-E-009-018-MY3.

References

[1] Dudley J M, Genty G and Coen S 2006 *Rev. Mod. Phys.* **78** 1135
[2] Xing Q, Zhang W and Yoo K M 1995 *Opt. Commun.* **119** 113
[3] Apolonski A, Povazay B, Unterhuber A, Drexler W, Wadsworth W J, Knight J C and Russell P S J 2002 *J. Opt. Soc. Am.* B **19** 2165
[4] Smektala F, Quemard C, Couderc V and Barthélémy A 2000 *J. Non-Cryst. Solids* **274** 232
[5] Zhan C, Zhang D, Zhu D, Wang D, Li Y, Li D, Lu Z, Zhao L and Nie Y 2002 *J. Opt. Soc. Am.* B **19** 369
[6] Petit L, Carlie N, Richardson K, Humeau A, Cherukulappurath S and Boudebs G 2006 *Opt. Lett.* **31** 1495
[7] Keller U *et al* 1996 *IEEE J. Sel. Top. Quantum Electron.* **2** 435
[8] Lin J H, Chen H R, Hsu H H, Wei M D, Lin K H and Hsieh W F 2008 *Opt. Express* **16** 16538
[9] Liu Y M and Prucnal P R 1993 *IEEE J. Quantum Electron.* **29** 2663
[10] Wang C, Zhang W and Yoo K M 1997 *J. Opt. Soc. Am.* B **14** 1881
[11] Tsang T 1993 *Opt. Lett.* **18** 293
[12] Lin J H, Wei M D, Hsieh W F and Wu H H 2001 *J. Opt. Soc. Am.* B **18** 1069
[13] Greene J M 1979 *J. Math. Phys.* **20** 1183
[14] Chen C H, Tai P T and Hsieh W F 2004 *Opt. Commun.* **241** 145
[15] Lin J H and Hsieh W F 2003 *Opt. Commun.* **225** 393
[16] Siegman A E 1986 *Lasers* (Mill Valley, CA: University Science Books)
[17] Chen C H, Wei M D and Hsieh W F 2001 *J. Opt. Soc. Am.* B **18** 1076
[18] Shieh J M, Ganikhanov F, Lin K H, Hsieh W F and Pan C L 1995 *J. Opt. Soc. Am.* B **12** 945
[19] Lin J H, Hsieh W F and Wu H H 2002 *Opt. Commun.* **212** 149
[20] Kutz J N, Collings B C, Bergman K and Knox W H 1998 *IEEE J. Quantum Electron.* **34** 1749
[21] Yariv A 1991 *Optical Electronics* (New York: Saunders College)
[22] Haus H A 1976 *IEEE J. Quantum Electron.* **12** 169
[23] Arecchi F T, Meucci R, Puccioni G and Tredicce J 1982 *Phys. Rev. Lett.* **49** 1217
[24] Weiss C O and Klische W 1984 *Opt. Commun.* **51** 47
[25] Weiss C O and Vilaseca R 1991 *Dynamics of Lasers* (Deerfield Beach, FL: VCH)
[26] Lugiato L A, Prati F, Naducci L M, Ru P, Tredicce J R and Bandy D K 1988 *Phys. Rev.* A **37** 3847
[27] Lugiato L A, Oppo G L, Tredicce J R, Narducci L M and Pernigo M A 1990 *J. Opt. Soc. Am.* B **7** 1019
[28] Alessandro G D and Oppo G L 1992 *Opt. Commun.* **88** 130
[29] Wu H H and Hsieh W F 2001 *J. Opt. Soc. Am.* B **18** 7
[30] Wu H H, Sheu C C, Chen T W, Wei M D and Hsieh W F 1999 *Opt. Commun.* **165** 225
[31] Tai P T, Hsieh W F and Chen C H 2004 *Opt. Express* **12** 5827
[32] Tai P T, Hsieh W F and Wu H H 2005 *Opt. Express* **13** 1679
[33] Moulton P F 1986 *J. Opt. Soc. Am.* B **12** 125
[34] Pinto J F, Esterowitz L, Rosenblatt G H, Kokta M and Peressini D 1994 *IEEE J. Quantum Electron.* **30** 2612
[35] Chen C H and Lin J H 2008 *Opt. Commun.* **281** 683
[36] Chen C H, Tai P T, Hsieh W F and Wei M D 2003 *J. Opt. Soc. Am.* B **18** 1220